

## In Situ Atomic Force Microscopy of the Mesomorphic–Monoclinic Phase Transition in Isotactic Polypropylene

René Androsch<sup>†</sup>

Center of Engineering Sciences, Martin-Luther-University  
Halle-Wittenberg, D-06099 Halle/S., Germany

Received October 21, 2007

Revised Manuscript Received December 23, 2007

**Introduction.** Melt-crystallization of isotactic polypropylene (iPP), in the absence of special nucleating agents, strongly depends on the applied rate of cooling. Slow cooling at rates lower than about  $10^2 \text{ K s}^{-1}$  leads to formation of stable monoclinic  $\alpha$ -crystals, and rapid cooling at rates between about  $10^2$  and  $10^3 \text{ K s}^{-1}$  leads to formation of a mesomorphic phase.<sup>1–3</sup> Further increase of the cooling rate yields a fully amorphous polymer as long as the temperature is kept below the glass transition at about 240–250 K.<sup>4</sup> The mesomorphic phase, at ambient temperature, is an arrested metastable structure, and irreversibly transforms on heating to stable monoclinic crystals, starting at about 350 K. The mesomorphic–monoclinic phase transition of rapidly cooled iPP was in the past frequently monitored and analyzed by temperature-resolved X-ray scattering and by calorimetry.<sup>5–8</sup> Direct, microscopic observation of the effect of the mesomorphic–monoclinic phase transition on the crystal morphology in bulk iPP still is lacking, and this is the subject of this communication.

At molecular level, the macromolecules adopt a  $3_1$  helix, in both mesomorphic and monoclinic phases.<sup>9,10</sup> At the supermolecular level, the lateral arrangement of left-handed and right-handed helices in the mesomorphic phase is random.<sup>11–13</sup> The mesomorphic phase develops on primary melt-crystallization at extremely large supercooling at about 290–310 K.<sup>2</sup> As a consequence, due to the high density of nuclei, the longitudinal and lateral size of mesomorphic domains is only 10–20 nm.<sup>14–18</sup> In the monoclinic phase, in contrast, left- and right-handed helices are in a defined sequence, forming layers.<sup>12</sup> Therefore, the lateral packing density of molecules is increased in the monoclinic structure.<sup>13</sup> Formation of the monoclinic phase on melt-crystallization occurs typically between about 350 and 390 K.<sup>2</sup> The crystals adopt a lamellar geometry, and they are organized in higher-order spherulitic superstructures.<sup>19,20</sup>

The exact mechanism of the mesomorphic–monoclinic phase transition on heating is not well-explored yet. It must involve in particular the rearrangement of helices of random handedness in the mesophase to ordered layers of helices of defined handedness in the monoclinic phase. In principle, the transition may occur by melting of mesomorphic domains, formation of a supercooled liquid, and subsequent recrystallization into the monoclinic structure. In this case, a change of the crystal size and shape is expected. Alternatively, the phase transition may proceed at local scale within existing domains, without complete melting. The morphology of the initially mesomorphic domains would then be preserved.

A review of the relevant literature does not provide unequivocal information about the path of transformation of the mesomorphic phase to the monoclinic phase, i.e., whether the

transformation occurs via the liquid state, or not. The majority of reports suggests preservation of the initially nodular geometry of the mesomorphic phase, pointing to a solid–solid-phase transformation.<sup>14,15,18,21</sup> This conclusion is indirectly derived from analysis of the crystal morphology at ambient temperature, after samples of initially quenched and mesomorphic iPP were annealed at a temperature higher than the temperature of the phase transition. Recently, and in contrast to the former research, a real-time study of homogeneous nucleation, growth, and phase transformation in strongly supercooled nanodroplets using atomic force microscopy seemed to provide direct evidence for complete reorganization of the morphology of initially mesomorphic domains as a consequence of the phase transformation during heating.<sup>22</sup> In detail, isolated homogeneous nuclei were detected on slow cooling of an initially strongly supercooled liquid of iPP at a temperature of about 308 K, which grew to an irregularly shaped, apparently branched object of size of several hundred nanometers. Subsequent heating to temperatures up to 353 K did not result in a change of the crystal shape, whereas further heating to 363 K revealed disintegration of the initially branched crystal and complete reorganization into a different crystal form at close to 373 K.

To further track the mechanism of the mesomorphic–monoclinic phase transformation on heating of initially rapidly cooled iPP, in situ atomic force microscopy was performed to observe the crystal morphology as a function of temperature. We intend to provide further evidence, in support of our former suggestion,<sup>3,21</sup> that in bulk mesomorphic iPP the phase transformation is not accompanied by a change of the morphology of crystals. The consequence of this conclusion is far reaching, since it implies that molecular segments in the mesophase are sufficiently mobile to undergo considerable conformational rearrangements.

**Experimental Section.** For the present study we used iPP with a molecular weight of  $373 \text{ kg mol}^{-1}$  and a polydispersity of 6.2, provided by Basell. The phase structure, the crystallization, and the melting behavior of this particular polymer are described in detail elsewhere.<sup>3,21,23</sup> Mesomorphic samples of about  $100 \mu\text{m}$  thickness were prepared using a special device for controlled rapid melt-crystallization, developed by Piccarolo.<sup>24</sup> The applied rate of cooling was  $1050 \text{ K s}^{-1}$ . Atomic force microscopy (AFM) was performed using a Quesant Q-Scope 250 microscope, equipped with a Quesant hot-stage and a  $40 \mu\text{m} \times 40 \mu\text{m}$  scanner. We used standard silicon cantilevers NSC16 with a force constant of  $40 \text{ N m}^{-1}$ , and a resonant frequency of about 150 kHz. Scanning was done in tapping mode. Dynamic differential scanning calorimetry (DSC), for evaluation of the temperature range of the mesomorphic–monoclinic phase transition of the particular iPP of the present study, was performed on a DSC 7 (Perkin-Elmer), using a rate of heating of  $10 \text{ K min}^{-1}$ .

**Results and Discussion.** Figure 1 shows AFM phase images recorded at ambient temperature and at 330, 364, and 398 K (from left to right). The top row provides an overview of the structure, and the bottom images are soft zooms that allow one to trace the morphology of preselected domains/crystals. As a guide for the eye, we inserted a rectangle which helps to identify identical objects in the various micrographs. For the sake of easy recognition of the temperature range of the mesomorphic–monoclinic phase transition we included at the bottom of Figure 1 a DSC heating scan. Heat-flow-rate raw data are converted

<sup>†</sup> Telephone: +49 3461 46 3762. Fax: +49 3461 46 3891. E-mail: rene.androsch@iw.uni-halle.de.

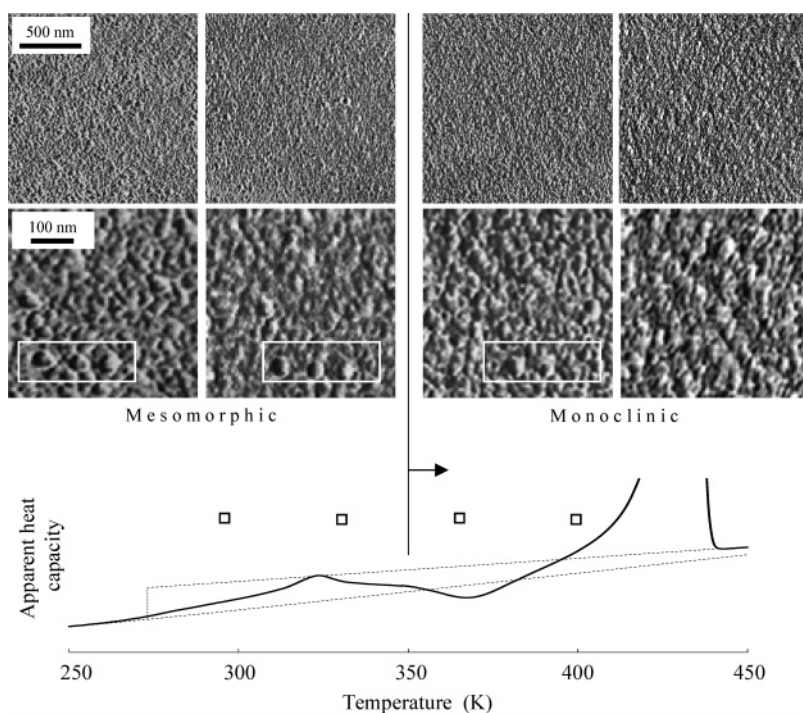


**Figure 1.** AFM phase images of initially rapidly cooled iPP, taken at ambient temperature, 330, 364, and 398 K (from left to right). The top images are of original size, and the bottom images are soft zooms. At the bottom is shown the apparent specific heat capacity of quenched iPP as a function of temperature, on heating at a rate of 10 K min<sup>-1</sup>. The squares indicate temperatures at which AFM images were taken. Further details are explained in the text.

to apparent specific heat capacities and are plotted as a function of temperature, together with heat-capacity data of fully crystalline and liquid iPP, as listed in the ATHAS data base (dotted lines).<sup>25</sup> The squares indicate temperatures at which AFM images were taken. The mesomorphic–monoclinic phase transition is an exothermic, thermally triggered transition. The phase transformation starts at about 350 K, which is indicated with the arrow in the DSC scan at the bottom of Figure 1, and which is confirmed by additional temperature-resolved X-ray analysis in a previous study.<sup>23</sup>

At ambient temperature and at 330 K, the initially quenched specimen consists of an amorphous phase and a mesomorphic phase. The corresponding AFM images show nodular domains with an average size of about 20 nm, being in agreement with independent studies using different instrumentation.<sup>13,14,18</sup> The shape and size of these domains do not change on heating to 364 and 398 K; i.e., the mesomorphic–monoclinic phase transition is not connected with a change of the crystal morphology. In addition, we are even able to trace selected objects in the micrographs, which were taken at different temperature, before and after the phase transformation (see rectangular frames in the bottom AFM images). This observation clearly suggests that the phase transformation occurs within existing domains, and is not connected with prior complete melting and subsequent recrystallization. Note that major, classical reorganization starts at about 400 K, which was detected by increasing size of crystals as result of annealing in previous AFM studies on the same polymer.<sup>3,21</sup> This, probably, is the reason that the selected objects, can no longer be identified in the image, which was taken at 398 K.

**Conclusions.** The present study suggests that the mesomorphic–monoclinic phase transition in iPP occurs at local scale within existing domains. Complete, global melting, or disintegration, respectively, of initially mesomorphic domains seems not to be a prerequisite for transformation of the initially random arrangement of left- and right-handed helices in the mesomor-

phic phase into a layerlike packing of left- and right-handed helices in the monoclinic phase. Local melting within existing domains, however, cannot be excluded, since a detection of such a process by analysis of the morphology of domains is impossible. The absence of complete disintegration of domains on heating indicates that there is sufficient rotational/torsional and/or positional mobility of helical stems in the mesomorphic phase at the temperature of the phase transition. If this is true, two options remain for the rearrangement of molecule structure at a local scale. Molecular stems in the mesomorphic phase either need to rewind to achieve a different handedness, as was observed in polytetrafluoroethylene<sup>26</sup> and poly( $\beta$ -phenylpropyl L-aspartate),<sup>27</sup> or need to move to a different position, without changing their handedness. The latter mechanism, i.e., preservation of the handedness of molecular stems during a solid–solid phase transformation has been identified in polybutene-1.<sup>28</sup> Figure 2 sketches these two mechanisms. It shows projections of mesomorphic (left) and monoclinic structure (right) of iPP on the (001) plane, with the white and black triangles representing different handedness of the stems. Lateral packing density of the stems in the mesophase is reduced, which allows additional free rotation around their molecular axis. The thermally triggered phase transformation is indicated with the horizontal arrow. The top and bottom illustrations visualize phase transformation via rewinding or translation of two molecules, respectively. The inclined lines show layers which finally only contain left- or right-handed helices. The densification of structure by additional vertical shifts along the molecular axis, or rotation, as required for interlocking of layers is not shown.

The experimental finding of considerable mobility of chains in mesomorphic iPP can further be discussed in terms of the liquid–crystal phase transformation in crystallizable polymers. A recently developed model suggests formation of crystals via a mesomorphic transient phase at the crystal growth front.<sup>29</sup> Without entering into the controversy about this model,<sup>30</sup> which

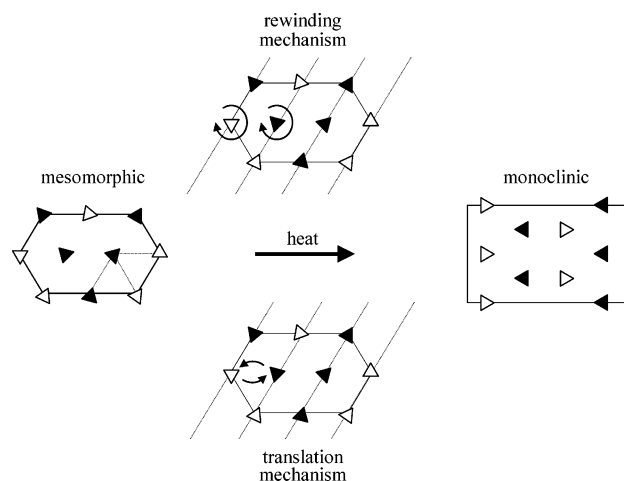


**Figure 2.** Model of the mesomorphic–monoclinic phase transformation in iPP. The illustrations are projections of mesomorphic (left) and monoclinic (right) iPP on the (001) lattice plane. The white and black triangles represent helices of different handedness. The transformation occurs on heating via a rewinding mechanism (top), or translation mechanism (bottom).

would be beyond the scope of this communication, the results of the present study indicate the technical but not necessarily the thermodynamic feasibility of such a transition at the crystal growth front.

**Acknowledgment.** The author thanks Qamer Zia (Martin-Luther-University Halle-Wittenberg, Germany) for measuring the AFM images. In particular, I thank Prof. Bernard Lotz (University of Strasbourg, France) for helpful discussion of this work. Financial support by the Ministry of Culture of Saxony-Anhalt (Germany) is gratefully acknowledged.

## References and Notes

- (1) Piccarolo, S. *J. Macromol. Sci. Phys.* **1992**, *B31*, 501–511.
- (2) De Santis, F.; Adamovsky, S.; Titomanlio, G.; Schick, C. *Macromolecules* **2006**, *39*, 2562–2567.
- (3) Zia, Q.; Androsch, R.; Radusch, H.-J.; Piccarolo, S. *Polymer* **2006**, *47*, 8163–8172.

- (4) Miyamoto, Y.; Fukao, K.; Yoshida, T.; Tsurutani, N.; Miyaji, H. *J. Phys. Soc. Jpn.* **2000**, *69*, 1735–1740.
- (5) Fichera, A.; Zannetti, R. *Makromol. Chem.* **1975**, *176*, 1885–1892.
- (6) Zannetti, R.; Celotti, G.; Fichera, A.; Francesconi, R. *Makromol. Chem.* **1969**, *128*, 137–142.
- (7) O’Kane, W. J.; Young, R. J.; Ryan, A. J.; Bras, W.; Derbyshire, G. E.; Mant, G. R. *Polymer* **1994**, *35*, 1352–1358.
- (8) Bodor, G.; Grell, M.; Kallo, A. *Faserforsch. Textiltech.* **1994**, *15*, 527–532.
- (9) Corradini, P.; Petraccone, V.; De Rosa, C.; Guerra, G. *Macromolecules* **1988**, *19*, 2699–2703.
- (10) Miller, R. L. *Polymer* **1960**, *1*, 135–143.
- (11) Natta, G.; Peraldo, M.; Corradini, P. *Rend. Accad. Naz. Lincei* **1959**, *26*, 14–17.
- (12) Natta, G.; Corradini, P. *Nuovo Cim. Suppl.* **1960**, *15*, 40–51.
- (13) Caldas, V.; Brown, G. R.; Nohr, R. S.; MacDonald, J. G.; Raboin, L. E. *Polymer* **1994**, *35*, 899–907.
- (14) Hsu, C. C.; Geil, P. H.; Miyaji, H.; Asai, K. *J. Polym. Sci., Polym. Phys.* **1986**, *24*, 2379–2401.
- (15) Wang, Z. G.; Hsiao, B. S.; Srinivas, S.; Brown, G. M.; Tsou, A. H.; Cheng, S. Z. D.; Stein, R. S. *Polymer* **2001**, *42*, 7561–7566.
- (16) Grubb, D. T.; Yoon, D. Y. *Polym. Commun.* **1986**, *27*, 84–88.
- (17) McAllister, P. B.; Carter, T. J.; Hinde, R. M. *J. Polym. Sci., Polym. Phys.* **1978**, *16*, 49–57.
- (18) Ogawa, T.; Miyami, H.; Asai, K. *J. Phys. Soc. Jpn.* **1985**, *54*, 3668–3670.
- (19) Binsbergen, F. L.; De Lange, B. G. M. *Polymer* **1968**, *9*, 23–40.
- (20) Olley, R. H.; Bassett, D. C. *Polymer* **1989**, *30*, 399–409.
- (21) Zia, Q.; Radusch, H.-J.; Androsch, R. *Polymer* **2007**, *48*, 3504–3511.
- (22) Kailas, L.; Vasilev, C.; Audinot, J.-N.; Migeon, H.-N.; Hobbs, J. K. *Macromolecules* **2007**, *40*, 7223–7230.
- (23) Androsch, R.; Wunderlich, B. *Macromolecules* **2001**, *34*, 5950–5960.
- (24) Androsch, R.; Wunderlich, B. *Macromolecules* **2001**, *34*, 8384–8387.
- (25) Androsch, R.; Wunderlich, B. *J. Polym. Sci., Polym. Phys.* **2003**, *41*, 2039–2051.
- (26) Brucato, V.; Piccarolo, S.; La Carubba, V. *Chem. Eng. Sci.* **2002**, *57*, 4129–4143.
- (27) Advanced THERMAL Analysis System; Wunderlich, B. *Pure Appl. Chem.* **1995**, *67*, 1019–1026.
- (28) De Rosa, C. *Macromolecules* **1988**, *21*, 1174–1176.
- (29) Watanabe, J.; Okamoto, S.; Satoh, K.; Sakajiri, K.; Furuya, H.; Abe, A. *Macromolecules* **1996**, *29*, 7084–7088.
- (30) Lotz, B.; Mathieu, C.; Thierry, A.; Lovinger, A. J.; Rosa, C. De; Ruiz de Ballesteros, O.; Auriemma, F. *Macromolecules* **1998**, *31*, 9253–9257.
- (31) Strobl, G. *Prog. Polym. Sci.* **2006**, *31*, 398–442.
- (32) European Discussion Meeting, Polymer Crystallization, Oct 03–06, 2007, Waldau, Germany; Hu, W.; Reiter, G., Organizers.

MA702334Q